Disordered Chain Conformations of Poly(tetrafluoroethylene) in the High-Temperature Crystalline Form I

Maddalena D'Amore, Finizia Auriemma,* Claudio De Rosa, and Vincenzo Barone

Dipartimento di Chimica, Università di Napoli Federico II, Complesso Monte Samt' Angelo, via Cintia, 80126 Napoli, Italy

Received June 14, 2004; Revised Manuscript Received September 14, 2004

ABSTRACT: Model conformations of polytetrafluoroethylene (PTFE) chains containing various amounts of helix reversal defects suitable for the high-temperature form I of PTFE have been modeled using semiempirical methods implemented in the Gaussian package, which makes use of the PM3 Hamiltonian. In these disordered conformations, ordered portions of chains in right- and left-handed 15/7 helical conformation succeed each other statistically along the chain. The Fourier transform of model chains containing various amounts of helix reversal defects obtained through the QM approach are then compared with the experimental X-ray fiber diffraction patterns of PTFE. Straight and slim model chains of PTFE containing helix reversal defects may be obtained at a low cost of internal energy and with small lateral encumbrance. For the minimum energy conformers the defect is always localized into a small region involving only 4 $-CF_2-$ units, with the internal variables placed at the junction between the two enantiomorphic portions of chain, deviating only slightly from their average values in the defect-free portions of chains. Two consecutive helix reversals do not interact with each other if they are separated by more than three dihedral angles, and their contributions to internal energy can be considered as additive. The energy cost is ∼2.3 kcal/mol for each reversal. The disordered conformations of PTFE chains account for the X-ray fiber diffraction patterns of form I of PTFE at temperatures higher than 30 °C. With increasing temperature an increase of the frequency of helix reversal defects is observed according to predictions of QM energy and Fourier transform calculations.

Introduction

Poly(tetrafluoroethylene) (PTFE) at atmospheric pressure shows a peculiar polymorphic behavior involving three crystalline phases as the temperature increases.[1] The three polymorphs are usually denoted as form II stable at temperatures lower than 19 °C, form IV stable at temperature between 19 and 30 °C, and form I stable at temperatures higher than 30 °C.[1] At 19 °C form II transforms into form IV, which in turn transforms into form I at 30 °C, resulting in a steplike increase of disorder in the crystals.[2]

The low-temperature form has been described in terms of a close packing of helical chains containing 13 CF_2 units in 6 turns, the dihedral angles only slightly deviating from the trans state ($T = 180°$).[3] Chains, in nearly 13/6 conformation, are packed in a nearly hexagonal lattice with $a' = b' = 5.59$ Å, $c = 16.9$ Å, and $\gamma' = 119.3°$.[4] Actually, the assumed commensurable 13/6 helix is slightly untwisted, giving rise to a noncommensurable helix.[2,5,6] According to refs 6−10 form II is characterized by rows of isomorphous helices alternating to rows of chains of opposite chirality in a nearly hexagonal arrangement (triclinic unit cell, two chains/unit cell).

The 19 °C transition from form II to form IV corresponds to slight untwisting of helical chains from 13/6 helix into 15/7 helix (15 CF_2 units in 7 turns).[2] At the onset of phase transition, the molecular packing changes from an ordered triclinic structure into a disordered hexagonal structure with larger interchain distances. The chain repetition of PTFE chains in form IV corresponds to $c = 19.5$ Å, and at 20 °C, the chain axes would be placed at the nodes of a hexagonal lattice with $a' = b' = 5.66$ Å. Extensive structural studies have indicated the presence of a large amount of structural disorder in form IV of PTFE. This disorder mainly consists of the occurrence of small angular displacements of chains around their axes and of a little translational disorder of chains parallel to their axes.[4] The chains are organized, at least in the short range, in rows of isomorphous helices packed with rows of chains of opposite chirality.[11−13]

At 30 °C form IV transforms into form I, which is characterized by the presence of larger amounts of disorder, the chain conformation becomes more irregular, and long-range order is maintained only in the parallelism of chain axes and in their pseudohexagonal arrangement.[4] The presence of conformational disorder, due to activation of helix reversals at temperatures higher than 30 °C, has been proposed.[13−21] In these disordered conformations ordered portions of chains in right-handed and left-handed 15/7 helical conformation succeed each other statistically along the chain. Evidence for the occurrence of helix reversal defects comes from IR spectroscopic studies[22] and X-ray diffraction experiments,[13,14,21,23] which indicate that the concentration of helix reversals increases with increasing temperature.

The effect of helix reversals on the X-ray diffraction intensity distribution in PTFE was first explicitly considered by Corradini et al. in ref 14. Helix reversals were modeled as sequences of torsion angle of the kind ...$T^+T^+T^+$ T $T^-T^-T^-$... $T^-T^-T^-$ T $T^+T^+T^+$... ($T^+ = -T^- = 165°$, T = 180°).

For these sequences of torsion angles the enantiomorphous helices are connected by at least one bond in the trans conformation. The shape of the chain remains

* To whom correspondence should be addressed. Phone: ++39 081 674341. Fax: ++39 081 674090. E-mail: Finizia.Auriemma@unina.it.

10.1021/ma0488257 CCC: $27.50
Published on Web 11/11/2004

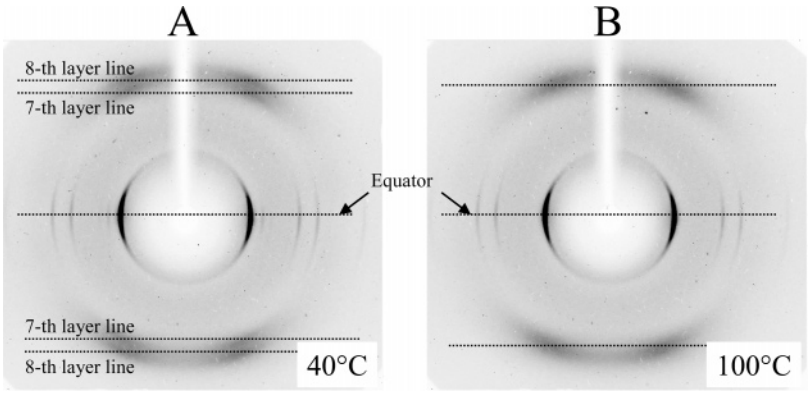

Figure 1. X-ray fiber diffraction patterns of a PTFE sample in Form I at 40 (A) and 100 °C (B). The diffuse scattering on the 7th and 8th layer lines at 40 °C (A) merge into a single diffuse halo, located on a line intermediate between the 7th and the 8th lines at 100 °C (B). (The X-ray diffraction patterns have been recorded using a KCCD Nonius automatic diffractometer, Mo Kα radiation monochromatized with a graphite single crystal.)

nearly unaltered with respect to the ordered one; moreover, the chain may be maintained exactly straight with small deformations of the torsion and bond angles with a low energetic cost.[14] Despite the conformational disorder a long-range three-dimensional order in the parallelism of the chain axes is maintained because the atoms are able to retain a fixed distance from the chain axis, so that the fluorine atoms are confined in a cylindrical envelope having the same size as in the ordered modification.[13,14,21]

It has been shown that the concentration of helix reversal defects increases steeply with temperature in the intermediate form, between 19 and 30 °C, and levels off in the high-temperature form as the temperature increases.[23] Dynamic scattering measurements have shown that PTFE chain segments have high mobility in the solid state as a consequence of the formation and motion of helix reversal defects. In the high-temperature form the reorientation of CF_2 groups occurs with rates in the range of 10−100GHz, whereas the presence of short-range orientational order in form IV leads to a slowing down of this motion.[23]

This paper is aimed at modeling defective conformations of PTFE chains containing helix reversals suitable for the high-temperature form of PTFE. Helix reversal defects have been widely modeled in the literature using empirical force fields. To overcome the limits of this classical approach we choose a quantum mechanical (QM) approach. In fact, while molecular mechanics (MM) methods produce minimum energy structures and packing arrangements consistent with experimental data, they can be inadequate whenever stereoelectronic effects play a significant role, as is possibly the case for electron-rich substituents such as fluorines. Therefore, a QM approach seems to be a more appropriate tool for chain conformation modeling in the case of fluoropolymers, where the conformational defects play an important role in determining the polymorphic behavior.

The Fourier transform of model chains containing various amounts of helix reversal defects obtained through the QM approach are compared with the experimental X-ray diffraction intensity distribution of oriented fibers of PTFE. A simple statistical model for the calculation of concentration of helix reversal defects as a function of the temperature is then attempted. This model, along with the comparison of calculated X-ray diffraction patterns with experimental diffraction profiles, allows one to set up the basis for a deeper understanding of disorder in form I of PTFE, originating from the presence of helix reversal defects, and conformational disorder in general.

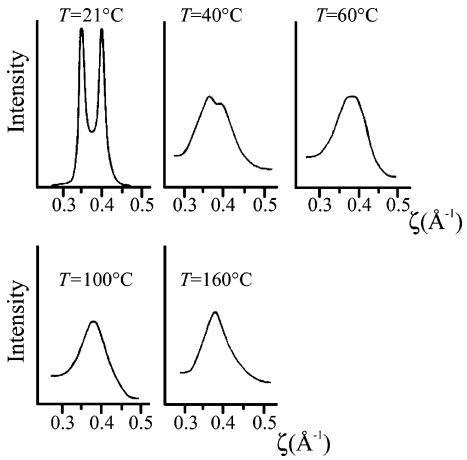

Figure 2. Experimental X-ray diffraction profiles of an uniaxially oriented PTFE sample at different temperatures.

X-ray Fiber Diffraction Patterns of High-Temperature Forms of PTFE. Accurate X-ray diffraction measurements on PTFE fibers at different temperatures, have revealed that form IV is characterized by three kinds of layer lines, those with a sharp spot only (equator and 15th layer lines), those with sharp spots and diffuse halos (7th and 8th layer lines), and those with diffuse halos only (all remaining layer lines);[4] at 30 °C transition the sharp spots disappear except for those on the equator and on the 15th layer line.[4]

X-ray diffraction patterns of form I present, indeed, sharp reflections only along the equator and the 15th layer line and diffuse halos in an intermediate region of the reciprocal space placed between the 7th and 8th layer lines.[4,24] At temperatures higher than 150 °C, the sharp peaks on the 15th layer line also disappear.[25]

The X-ray fiber diffraction patterns of form I of PTFE at 40 and 100 °C are reported in Figure 1 as an example. The diffuse scattering located on the 7th and 8th layer lines present at 40 °C (Figure 1A) merge into a single broad halo centered on a layer line placed between the 7th and 8th layer lines in the diffraction pattern at 100 °C (Figure 1B).

The experimental X-ray diffraction profiles of uniaxially oriented PTFE fibers recorded at different temperatures are reported in Figure 2 as a function of the reciprocal coordinate ζ, redrawn from ref 21. The value of the reciprocal coordinate ξ is fixed close to the position

of maximum intensity on the 7th and 8th layer lines. It is apparent from Figure 2 that, while below 30 °C the 7th and 8th layer lines are well defined, with increasing temperature the two layer lines become ill defined and approach each other, merging into a single broad layer line centered between; with further increase of temperature (up to 160 °C) the profile of the single-layer line becomes increasingly narrow. This behavior could be explained as due to a thermally activated process leading to an increase of concentration of helix reversals as the temperature increases.[14,21]

Calculation Method

Conformational Analysis. As a starting point we studied a single chain of poly(tetrafluoroethylene) (PTFE) by one of the semiempirical methods implemented in the Gaussian package,[26] which makes use of the PM3 Hamiltonian.[27,28]

This semiempirical method, based on the neglect of differential overlap approximation (NNDO), has been parametrized to provide good geometries and heat of formation for a large set of molecules containing elements of the second and third rows of the periodic table. In particular, conformational features are described quite well thanks to an improved representation of nonbonded interactions.[29]

Minimum energy conformations have been obtained in the case of aperiodic model oligomers containing different numbers of helix reversal defects and, for comparison, in the case of periodic 13/6 and 15/7 helices typical of form II and forms IV and I of PTFE, respectively.

In the case of aperiodic model conformations, the internal energy has been minimized with respect to all internal variables, provided that the conformations of the starting model were sufficiently straight and elongated. In the case of periodic chain models, instead, during the minimization the backbone bonds, valence angles, and backbone dihedral angles were kept fixed whereas only the positions of fluorine atoms were left free to relax.

More precisely, we performed geometry optimizations on model chains of perfluorooligomers $CF_3(-CF_2-)_{n-2}\ CF_3$ with $n = 4-64$ starting from the all-trans conformation. The optimized chain models obtained by this procedure contain a number of helix reversal defects depending on the length of oligomer. In fact, for sufficiently long oligomers ($n \geq 10$) we found minima showing at least a single helix reversal along the chain; in the case of $n = 64$, the optimization procedure converges to a model containing seven inversions (one reversal every nine CF_2 groups on average). Then for the longest optimized model oligomer (containing seven reversals) the number of helix reversals has been gradually decreased down to zero, obtaining model oligomers with 6, 5, ..., and 0 reversals, and each conformer has been further optimized, obtaining minimum energy conformations going from the defect-free chain to those containing (on average) one reversal every 64, 32, 21, 16, 13, 11, and 9 CF_2 groups. Generally, if two consecutive reversals were displaced by at least three C−C bonds, the minimized conformers included the same number of helix reversals and in the same positions as in the starting conformations. For each conformer with a given number of reversals, at least three independent minimum energy model conformers have been obtained all characterized by nearly the same energy but a different distribution of the length of the individual helical portions.

The periodic 13/6 and 15/7 helices considered in our calculations correspond to conformers with 64 carbon atoms having C−C bond lengths and C−C−C valence angles equal to the average values (1.60 Å and 110.05°, respectively) found by means of PM3 optimizations over all internal variables on the defect-free aperiodic helical oligomers; the C−C−C−C dihedral angles, instead, have been fixed equal to values that reproduce the unit height and the unit twist of crystalline form II and form IV of PTFE proposed by Clark in a recent paper.[6] We recall that for a *M*/*N* helix, including *M* repeating units in a period of *N* turns, the unit height and unit twist are defined as $h=c/M$ (c = chain axis and M = number of CF_2 units in a period) and $t = 2\pi N/M$.[30] Assuming for the 13/6 helix $h = 1.30$ Å and $t = 166.15°$ ($c = 16.9$ Å),[6] the C−C−C−C dihedral angles are all equal to +163° and −163° for the right- and left-handed helices, respectively. Assuming for the 15/7 helix $h = 1.30$ Å and $t = 168°$ ($c = 19.5$ Å),[6] the C−C−C−C dihedral angles are all equal to +166° (right-handed) and −166° (left-handed helix).

X-ray Diffraction Modeling. Fourier transform calculations have been performed on isolated chains containing different numbers of helix reversal defects. Our proposed models lack any periodicity in the individual helical stems and are suitable for description of the disordered conformation of form I at high temperature. The transition from form IV into form I has been indicated as a transition between a disordered state controlled by intra- and intermolecular forces into one which is only determined by intramolecular potentials.[4,23] Authors agree that in form I, at high temperature, any residual translational order parallel to chain axes and orientational order around chain axes is lost (see, for instance, refs 4, 12, 13, 23). Since there are no lateral correlations between the chains, the only order being the positioning of the chain axes on the hexagonal lattice, the packing influence on the conformation may be neglected. The Fourier transform of isolated chains may be advantageously compared to the diffracted intensity far from the equator when there is a low degree of rotational (around the chain axis) and translational (along the chain axis) order between adjacent parallel chains.

The X-ray diffraction profiles discussed in the following have been calculated as a function of the cylindrical coordinates ξ and ζ in the regions of reciprocal space corresponding to $\xi = 0$, $0.4 < \zeta < 1$ Å^{-1} (i.e., along the meridian), and for $\xi = 0.18$ Å^{-1}, $0.15 < \zeta < 0.55$ Å^{-1}, because in these regions the experimental X-ray diffraction patterns of form I of PTFE present the most important information regarding the possible conformational disorder.

The square modulus of the structure factor (I_c), to be compared with the experimental X-ray fiber diffraction intensity (I), was calculated using the following formula

$$I_c = \sum_{i,j} C_{ij} g_{ij} \tag{1}$$

The factors (C_{ij}) in eq 1 account for the interference between couples of atoms i and j

$$C_{ij} = f_i f_j J_0(2\pi\xi r_{ij}) \exp(2\pi\zeta z_{ij}) \tag{2}$$

The second term (g_{ij}) accounts for the finite length of the chains and is of the type[31]

$$g_{ij} = (1 - 2p_c)^{|z_{ij}|/\Delta l} \tag{3}$$

In eq 1 the interference of atoms in 34 consecutive monomeric units in a chain (atomic coordinates x_i, y_i, z_i, atomic scattering factors f_i) with the remaining atoms along the chain (atomic coordinates x_j, y_j, z_j; atomic scattering factors f_j) is considered. In he eq 2 $r_{ij} = [(x_i - x_j)^2 + (y_i - y_j)^2]^{1/2}$ and $z_{ij} = (z_i - z_j)$ are the distances in the xy plane and along z, respectively, between atoms i and j, and J_0 is the zeroth-order Bessel function.[32] In eq 3 Δl is the average axial advance per monomeric unit (see Table 1), p_c represents a Bernoulli-type probability that the chain ends up growing along the chain axis on every addition of a new CF_2 unit, $\Delta l/p_c$ is the average correlation length of the chain.[33] In the calculations the value of $\Delta l/p_c$ has been fixed equal to 20 Å to reproduce the broadening along ζ of the experimental diffraction peaks.

The average value of the diffraction intensity was calculated by choosing, for each reciprocal point (ξ,ζ), the reference sequence of 34 consecutive monomeric units at random in the central region of the oligomer with $n = 64$, discarding the eight terminal CF_2 units at both ends. This allows averaging the calculated intensity over conformers having different distributions of the length of the individual helical stems, so that the

Table 1. Average Distance Along the Chain Axis between Consecutive $-CF_2-$ Units (Δl), Values of the Mean ($\langle s \rangle$) and Root-Mean-Square ($\langle s^2 \rangle^{1/2}$) of the Lateral Encumbrance, and Energy Contributions for Each Reversal of Different Conformers with Increasing Number of Defects (m). For Comparison, the Values of the $\langle s \rangle$ Parameter (coinciding with $\langle s^2 \rangle^{1/2}$) Are Collected for Periodic Helices

m	$\Delta E_i/m$ (kcal/mol)	$\langle s \rangle$ (Å)[a]	$\langle s^2 \rangle^{1/2}$ (Å)[b]	Δl (Å)
0	0	1.68	1.68	1.29
1	2.32	1.67	1.68	1.29
2	2.31	1.69	1.71	1.29
3	2.31	1.67	1.68	1.29
4	2.32	1.78	1.86	1.28
5	2.32	1.77	1.84	1.29
6	2.28	1.94	2.09	1.28
7	2.32	1.93	2.06	1.28

	$\langle s \rangle$[a]	h (Å)[c]	ΔE (kcal/mol)[d]
13/6 helix	1.67	1.30	~0.007
15/7 helix	1.67	1.30	0.078

[a] Calculated according to eq 4. [b] Calculated as the square root of eq 5. [c] Unit height. [d] Energy difference with respect to the defect-free helix minimized with respect to all internal variables.

result of Fourier transform is independent of the particular model of the conformation adopted in the calculations. We checked that in the regions of reciprocal space of interest for our calculation the same results are obtained by a classical averaging of the calculations of the Fourier transforms of different oligomer models having a different distribution of length of individual helical portions. Our calculation technique implies a short computation time and avoids the appearance in the calculated X-ray diffraction profiles of spurious maxima due to termination effects.

Results and Discussion

In previous studies helix reversals have been modeled in the simplifying hypotheses that two consecutive enantiomorphic helical portions of chains are joined by means of at least one dihedral angle in the trans state and in the hypothesis that the dihedral angles in the right- and left-handed portions of chains remain all equal to the values assumed by the ideal 15/7 helical chain in the crystalline state.[13,14,21] These assumptions were introduced in order to ensure that the atoms aside the defect are in registry with atoms of the surrounding chain and to prevent chains from bowing, thus avoiding large lattice distortions. At high temperatures a high amount of conformational disorder is present in form I of PTFE. Therefore, these assumptions seem unnecessary to build up conformationally disordered model chains of PTFE including helix reversals.

For this reason in our calculations the internal energy of model oligomers of PTFE has been minimized with respect to all internal coordinates. The obtained minimum energy conformations have backbone dihedral angles in nondefective right- and left-handed sequences displaced by at most ±2° from the average values of +161.95° and −161.95°, respectively, and the backbone valence angles are all nearly equal to 110.05° (from a minimum value of 109.32° to a maximum value of 112.3°).

Our models, independent of the length of model oligomer used in the calculations, are characterized, for each junction between two consecutive helical segments of opposite chirality, by the presence of a single C−C−C valence angle wider by about 2° (112.13°) than the value of 110.05° and of two dihedral angles at reversal

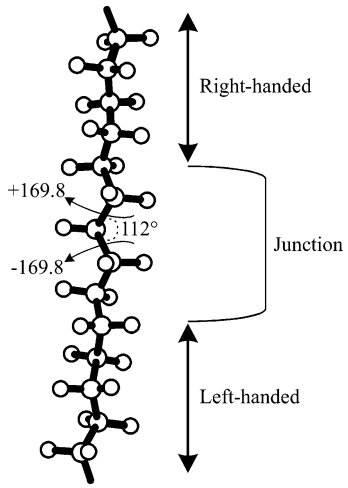

Figure 3. Typical minimum energy portion of PTFE chains including one helix reversal.

interface ~|8|° larger than the value of |161.95|° of the nondefective chain segments. Therefore, helix reversal defects are always localized into a small region involving four $-CF_2-$ units only and may be described, on average, by sequences of the kind +161.95° +161.95° +161.95° +169.84−169.84° −161.95° −161.95° −161.95° −169.85° +169.85°+161.95° +161.95°. These small deviations make helix reversals possible with a relatively low energy cost. A typical minimum energy portion of PTFE chains including one helix reversal is shown in Figure 3.

For the longest model oligomer $CF_3-(CF_2)_{62}-CF_3$ eight minima have been obtained corresponding to models with energy increasing from the defect-free chain to the models containing, in the order, one reversal every 64, 32, 21, 16, 13, 11, 9 CF_2 groups.

Regardless of the length of model oligomer, the energy cost of a single helix reversal of kind ...$T^+T^+T'^+T'^-T^-T^-T^-$... ($T^+ = -T^- = +162° \pm 2°$ and $T'^+ = -T'^- = +169.8° \pm 2°$) amounts to $\Delta E \approx 2.3$ kcal/mol with respect to the defect-free minimum energy model.

The effect of the simultaneous presence of two reversals (twin reversal) into a PTFE model oligomer on the conformational energy and their possible reciprocal interactions has been estimated building up sequences of kind ...$T^+T^+T^+(T^-)_nT^+T^+T^+$... (...$T^-T^-T^-(T^+)_nT^-T^-T^-$...), that is, introducing left- (right-) handed sequences of n dihedral angles into an otherwise fully right- (left-) handed chain oligomer. Calculations show that it is not possible to have helical sequences embedded into helical portions of opposite chirality of this kind for $n = 1$ or 2 since these structures converge to the defect-free minimum. For $n \geq 4$ the penalty for a twin helix reversal is doubled (4.6 kcal/mol) with respect to the energy cost of a single defect helix reversal (i.e., of kind ...$T^-T^-T^-T^+T^+T^+$... or ...$T^+T^+T^+$ $T^-T^-T^-$...), whereas when $n = 3$ the energy cost for a twin helix reversal is 0.32 kcal/mol higher than 4.62 kcal/mol and amounts to 4.94 kcal/mol. Therefore, it is possible to assume that two consecutive helix reversals separated by more than three dihedral angles do not interact with each other and their contributions to internal energy can be considered as additive.

In the obtained models the helical stems between consecutive inversions are not necessarily periodic since the sequence of backbone torsion angles is not regular but have values, after minimization, variable in the

range 162 ± 2°. It is reasonable to assume that these models are suitable for description of the disordered conformation of form I at high temperatures, whereas at 30 °C the helical portions are probably close to the periodic 15/7 conformation.

Table 1 collects the energy differences for the various minimum energy conformations exhibiting an increasing number of defects (from 1 to 7) with respect to the defect-free minimum energy conformation. In Table 1, for each conformation, the average distance along the chain axis between consecutive $-CF_2-$ units (Δl) and the values of the mean and root-mean-square lateral encumbrance ($\langle s \rangle$ and $\langle s^2 \rangle^{1/2}$, respectively) are also reported. The latter parameters correspond to the first ($\langle s \rangle$) and square root of the second moment ($\langle s^2 \rangle^{1/2}$) of the distribution function of the distances of fluorine atoms from the chain axis in a given disordered conformation and have been calculated using the following equations

$$\langle s \rangle = (n(F))^{-1} \sum_{i=1}^{n(F)} ({x_i}^2 + {y_i}^2)^{1/2} \quad (4)$$

$$\langle s^2 \rangle = (n(F))^{-1} \sum_{i=1}^{n(F)} ({x_i}^2 + {y_i}^2) \quad (5)$$

with $n(F)$ being the number of fluorine atoms in the model chains and x_i and y_i their $x-y$ coordinates with respect to an orthogonal frame having the z-axis coinciding with the chain axis.

It is apparent that at the PM3 level the estimated energy penalty for each helix reversal due to intramolecular effects is ~2.3 kcal/mol. This value is 0.6 kcal/mol higher than the corresponding value calculated by Farmer[34,35] but also higher than the experimental data for the formation energy for a single helix reversal, deduced from infrared absorption intensities, $\Delta E \approx 1.25$ kcal/mol.[22]

All conformers appear straight and of cylindrical shape (see Figure 3). The average distance along the chain axis between consecutive $-CF_2-$ units ($\Delta l = 1.29$ Å) is close to the unit height of the periodic 15/7 helix (1.30 Å). The lateral encumbrance of conformers increases as the concentration of defects increases, resulting in 1.68 Å in the case of the defect-free conformer, 1.93 Å for the conformer with the highest concentration of defects. The ratio between the root-mean-square and the mean values of lateral encumbrance in all cases is <1.1, indicating that all conformers are not bowed. Moreover, the radius of the average cylindrical envelope wrapping the conformer with the largest value of $\langle s \rangle$ is close to 2.6 Å (i.e., 1.93 + 0.67 = 2.6 Å, with 0.67 Å being the van der Waals radius of fluorine atoms). The latter value is still lower than one-half the distance between the first neighboring PTFE chains in the crystalline form I (equal to 5.66/2 Å = 2.83 Å at 30 °C).[6]

For comparison the internal energy in the case of periodic 13/6 and 15/7 helices has been also evaluated, fixing all internal variables of the skeletal chain to the values specified in the preceding section and minimizing the structures at the PM3 level only for the positions of the fluorine atoms. These results indicate that the 13/6 helix is 0.071 kcal/mol (of CF_2 units) lower than the 15/7 helix, consistent with the fact that at lower temperatures the conformation adopted by PTFE macromolecules in the crystalline state corresponds to helices with

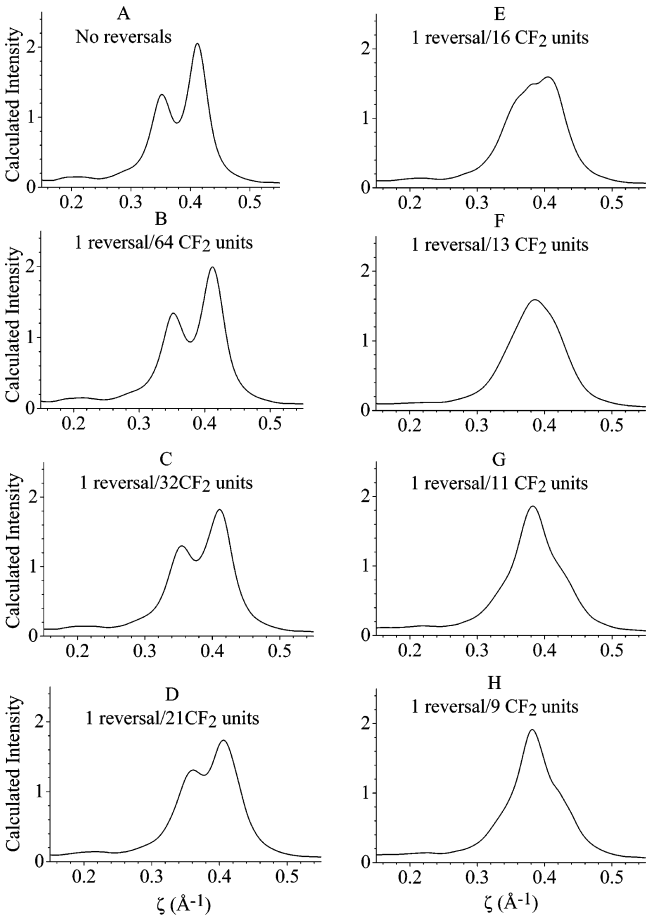

Figure 4. Calculated X-ray diffraction profiles at $\xi = 0.18$ Å^{-1} for 0.15 Å^{-1} < ζ < 0.55 Å^{-1} (i.e., the same region of reciprocal space as the experimental patterns of Figure 2) for model chains containing different concentrations of helix reversals: (A) No reversal; (B) 1 reversal every 64 CF_2 units; (C) 1 reversal every 32 CF_2 units; (D) 1 reversal every 21 CF_2 units; (E) 1 reversal every 16 CF_2 units; (F) 1 reversal every 13 CF_2 units; (G) 1 reversal every 11 CF_2 units; (H) 1 reversal every 9 CF_2 units.

M/*N* close to 13/6. Moreover, the periodic (13/6) and the nonperiodic (nph) helices corresponding to our lowest minimum are nearly isoenergetic ($\Delta E_{13/6-nph}$ (for 1 mol of CF_2 groups) ≈ 0.0070 kcal) and have nearly identical lateral encumbrance.

Fourier Transform Calculations. As discussed in the previous section, the X-ray fiber diffraction patterns of PTFE in the temperature range 20−160 °C indicate that the amount of structural disorder not only increases at the 30 °C transition, going from form IV to form I, but also in form I with increasing temperature. In fact, as shown in Figure 2, the two intense reflections on the seventh and eighth layer lines, typical of the 15/7 conformation in form IV gradually approach each other with increasing temperature and finally merge into a single-layer line over the temperature range 100−160 °C, becoming increasingly narrow. This behavior has been ascribed to an increase of concentration of helix reversal defects.[13,14,21,23]

In Figure 4 the calculated X-ray diffraction profiles for model chains containing different concentrations of helix reversals are shown.

The diffraction intensity has been calculated in the same regions of the reciprocal space as the experimental patterns of Figure 2, i.e., at $\xi = 0.18$ Å^{-1} for 0.15 Å^{-1} < ζ < 0.55 Å^{-1}, in the case of the model chain oligomers

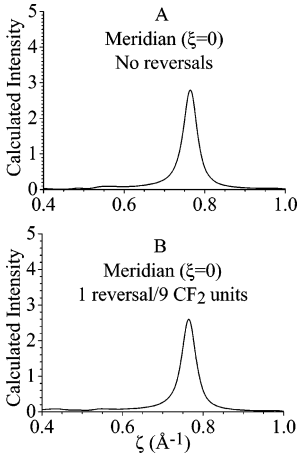

Figure 5. Calculated X-ray diffraction profiles along the meridian (at $\xi = 0$) for model chains with (A) no reversals and (B) 1 reversal every 9 CF_2 units.

of PTFE containing on average 1 helix reversal every 64, 32, 21, 16, 13, 11, and 9 CF_2 units (Figure 4B−H) and in the case of the defect-free model oligomer (Figure 4A). The calculated X-ray diffraction profile in the case of the defect-free oligomer has two distinct maxima at $\zeta(=l/c) = 7/19.5$ and $8/19.5$ Å^{-1} (Figure 4A); these maxima become broader and tend to approach each other as the concentration of helix reversals increases from 1/64 to 1/21 (Figure 4B−D) and merge into a single broad peak when the helix reversal concentration amounts to 1/16 (Figure 4E). With further increasing concentration of helix reversal defects, the diffraction peak in this section of reciprocal space becomes narrower (Figure 4F−H, helix reversal concentration 1/13−1/9). Therefore, a single-layer line is obtained for the minimum energy conformations containing about one reversal every 16 CF_2 groups, i.e., for a critical value of defects concentration $D \approx 1/16 = 0.127/CF_2$ units.

It is apparent that the presence of 1 reversal every 21 and 9 CF_2 units (Figure 4D and H, respectively) could account for the experimental patterns of form I at low (30−40 °C) and high (160 °C) temperatures (Figure 2), respectively. Moreover, the coalescence of the two diffraction maxima on the 7th and 8th layer line into a single diffraction peak at intermediate values of ζ, observed in the range of temperatures of 100−160 °C in Figure 2, occurs for a critical concentration of helix reversal defects close to 1 reversal every 16 CF_2 units (Figure 4E).

It is worth noting that the calculated X-ray diffraction patterns of all model oligomers of PTFE considered here have a strong diffraction peak along the meridian ($\zeta = 0$) at $\zeta = 15/c$, as shown, for example, in Figure 5 in the case of the defect-free model chain (Figure 5A) and for the model oligomer containing 1 reversal per 9 CF_2 units (Figure 5B). This indicates that the presence of helix reversals, according to our model, does not destroy the average chain periodicity, in agreement with the experimental data.

Statistical Model. Zero-point energy and thermal contributions to thermodynamic functions were computed from the PM3 structures and harmonic frequencies by using the rigid rotor/harmonic oscillator approximation and the standard expressions for an ideal gas in *PVT* ensemble at 298.15 K and 1 atm. The evaluated enthalpy for a single reversal in a chain of PTFE is $\Delta H_r = 2.18$ kcal/mol.

On the basis of the results of the previous analysis, we assume that sequences of dihedral angles not containing any reversal, of kind ...$T^{\pm}T^{\pm}T^{\pm}T^{\pm}$..., have energy zero, sequences containing a single helix reversal, of kind ...$T^{\pm}T^{\pm}(T'^{\pm}T'^{\mp})T^{\mp}T^{\mp}$..., have energy 2.18 kcal/mol, sequences containing two helix reversals separated by at least three bonds, of kind ... $T^{\pm}T^{\pm}(T'^{\pm}T'^{\mp})(T^{\mp})_i(T'^{\mp}T'^{\pm})T^{\pm}T^{\pm}$... ($i \geq 1$), have energy 4.36 kcal/mol (2(2.18) kcal/mol, we neglect the calculated extra energy amount equal to 0.32 kcal/mol when $n = 1$); those having three nonconsecutive helix reversals, of kind ...$T^{\pm}T^{\pm}$ $(T'^{\pm}T'^{\mp})(T^{\mp})_i(T'^{\mp}T'^{\pm})(T^{\pm})_j(T'^{\pm}T'^{\mp})T^{\mp}T^{\mp}$... ($i,j \geq 1$), have energy 6.54 kcal/mol (3(2.18) kcal/mol), etc., whereas sequences having consecutive helix reversals, of kind ...$T^{\pm}T^{\pm}(T'^{\pm}T'^{\mp}T'^{\pm})T^{\pm}T^{\pm}$... or ...$T^{\pm}T^{\pm}(T'^{\pm}T'^{\mp})$-$(T'^{\mp}T'^{\pm})T^{\pm}T^{\pm}$..., are forbidden.

The partition function of a chain constituted by N skeletal bonds susceptible to include helix reversal defects with the above listed restraints may be calculated using a matrix formalism if we associate to each couple of consecutive triplets of bonds in the chain a matrix **U** whose elements are the statistical weights of all possible states of the triplet of bonds in question with respect to all possible states of preceding triplet of bonds in the chain. Let us assume statistical weight 1 when a sequence of kind $T^{\pm}T^{\pm}T^{\pm}$ is succeeded by a bond in the state $T^{\pm}$, statistical weight $p = \exp(-\Delta E_r/RT)$ when a sequence of kind $T^{\pm}T^{\pm}T^{\pm}$ is succeeded by a bond in the state $T^{\mp}$, statistical weight 1 when a sequence of kind $T^{\pm}T^{\pm}T^{\mp}$ is succeeded by a bond in the state $T^{\mp}$, statistical weight 0 when a sequence of kind $T^{\pm}T^{\pm}T^{\mp}$ is succeeded by a bond in the state $T^{\pm}$, statistical weight 1 when a sequence of kind $T^{\pm}T^{\mp}T^{\mp}$ is succeeded by a bond in the state $T^{\mp}$, statistical weight 0 when a sequence of kind $T^{\pm}T^{\mp}T^{\mp}$ is succeeded by a bond in the state $T^{\pm}$. The statistical weight matrix may be written as (for more details see the Appendix)

$$\mathbf{U} = \begin{vmatrix} 1 & p & 0 \\ 0 & 0 & 1 \\ 1 & 0 & 0 \end{vmatrix} \tag{6}$$

The partition function corresponds to the product of matrixes[36]

$$Z \approx |1 \;\; 0 \;\; 0| \mathbf{U}^{N-2} \begin{vmatrix} 1 \\ 1 \\ 1 \end{vmatrix} \tag{7}$$

For the infinite chain, i.e., $N \gg 1$, the partition function of this system may be approximated by the maximum eigenvalue, λ, of the **U** matrix raised to the N power.[36]

$$Z \approx \lambda^N \tag{8}$$

Therefore, at a given temperature the equilibrium concentration of helix reversal defects (D) may be calculated using the equation[36]

$$D = \frac{\partial \ln Z}{\partial \ln p} \approx \frac{\partial \ln \lambda}{\partial \ln p} \tag{9}$$

Introducing into eq 9 the critical value of D for which the two diffraction maxima on the 7th and 8th layer line merge into a single peak estimated in the calculations of Figure 4 ($D = 1/16$, Figure 4E) and the ΔH_r values reported above ($p = \exp(-\Delta H_r/RT)$), we foresee that this coalescence corresponds to a critical temper-

$\mathbf{U}_{8X8}$ =

	$T_{i-1}{}^{+}T_i{}^{+}T_{i+1}{}^{+}$	$T_{i-1}{}^{+}T_i{}^{+}T_{i+1}{}^{-}$	$T_{i-1}{}^{+}T_i{}^{-}T_{i+1}{}^{+}$	$T_{i-1}{}^{+}T_i{}^{-}T_{i+1}{}^{-}$	$T_{i-1}{}^{-}T_i{}^{+}T_{i+1}{}^{+}$	$T_{i-1}{}^{-}T_i{}^{+}T_{i+1}{}^{-}$	$T_{i-1}{}^{-}T_i{}^{-}T_{i+1}{}^{+}$	$T_{i-1}{}^{-}T_i{}^{-}T_{i+1}{}^{-}$
$T_{i-2}{}^{+}T_{i-1}{}^{+}T_i{}^{+}$	1	p	0	0	0	0	0	0
$T_{i-2}{}^{+}T_{i-1}{}^{+}T_i{}^{-}$	0	0	0	1	0	0	0	0
$T_{i-2}{}^{+}T_{i-1}{}^{-}T_i{}^{+}$	0	0	0	0	0	0	0	0
$T_{i-2}{}^{+}T_{i-1}{}^{-}T_i{}^{-}$	0	0	0	0	0	0	0	1
$T_{i-2}{}^{-}T_{i-1}{}^{+}T_i{}^{+}$	1	0	0	0	0	0	0	0
$T_{i-2}{}^{-}T_{i-1}{}^{+}T_i{}^{-}$	0	0	0	0	0	0	0	0
$T_{i-2}{}^{-}T_{i-1}{}^{-}T_i{}^{+}$	0	0	0	0	1	0	0	0
$T_{i-2}{}^{-}T_{i-1}{}^{-}T_i{}^{-}$	0	0	0	0	0	0	p	1

(A-1)

ature of $T \approx 450$ K. This value is slightly higher than the upper limit, which could be estimated from the experimental X-ray diffraction patterns of Figure 2, which indicates that the critical temperature is in the range $373 < T < 433$ K. At $T = 430$ K, indeed, our model foresees one junction every 18 CF_2 units, which within our rough estimation of critical frequency of helix reversal defects is still in agreement with experimental data. The disagreement may be due to the fact that, as stated above, the PM3 Hamiltonian slightly overestimates the energy cost per helix reversal defect.

Conclusions

The disordered conformation of PTFE chains in form I has been studied. Defective conformations of PTFE chains containing helix reversals have been modeled using a QM approach. Geometry optimizations have been performed minimizing the energy of model oligomers with respect to all internal variables. Model chains of perfluorooligomers $CF_3-(CF_2)_{n-2}-CF_3$ with $n = 4-64$ have been considered. The results of the present analysis indicate that straight and slim model chains of PTFE containing helix reversal defects may be obtained at a low cost of internal energy and with small lateral encumbrance without introducing at the junction between consecutive enantiomorphic portions of chains any dihedral angle in the trans conformation, as assumed in the previous literature models. Moreover, at high temperature the helical portions of chains aside the defect may not be necessarily periodic 15/7 helical.

For the minimum energy conformers, independent of the length of model oligomer and the frequency of helix reversal defects present therein, the defect is always localized into a small region involving only four $-CF_2-$ units. The internal variables placed at the junction between the two enantiomorphic portions of chain deviate only slightly from their average values in the defect-free portions of chains. According to this analysis these junctions may be described, on average, by sequences of the kind ...$T^+T^+T^+$ ($T'^+T'^-$) $T^-T^-T^-$... (...$T^-T^-T^-$ ($T'^-T'^+$) $T^+T^+T^+$...) with $T^+ = -T^- = +162° \pm 2°$ and $T'^+ = -T'^- = +169.8° \pm 2°$. Two consecutive helix reversals do not interact each other if they are separated by more than three dihedral angles, and their contributions to internal energy can be considered as additive. The energy cost amounts to ~2.3 kcal/mol for each reversal and corresponds to an enthalpy of ~2.18 kcal/mol.

Calculations of Fourier transforms of the chain models obtained by energy analysis indicate that these models of helix inversion account for the experimental X-ray fiber diffraction patterns of form I of PTFE at temperatures higher than 30 °C.

The results of Fourier transform calculations indicate that irregular conformations, not containing helix reversals and with $-CF_2-$ groups projecting along the chain axis at an average distance of ~1.30 Å, are sufficient to account for the presence of broad diffraction halos on the 7th and 8th layer line in the diffraction patterns and for a strong Bragg peak on the 15th layer line, along the meridian. The presence of helix reversal defects induces a gradual coalescence of the diffuse scattering located on the 7th and 8th layer line into a single diffraction halo, centered in between, as their concentration increases. This coalescence occurs when the helix reversal concentration reaches the critical value of ~1 inversion per 16 CF_2 units. These results are in agreement with the experimental coalescence of the scattering on the 7th and 8th layer lines observed in the diffraction patterns with increasing temperature in the range 30−160 °C. The critical concentration of defects may be related through a statistical model to a critical value of the temperature. The so-estimated critical parameter is in agreement with the experimental value of the temperature at which the coalescence of diffuse scattering is observed in the experimental diffraction patterns.

The present analysis indicates that the QM minimum energy conformations modeled here are appropriate for the description of the chain conformation of PTFE in the crystalline form I stable at high temperature.

Appendix

Let us number the main chain dihedral angles from 1 to N. Actually, the statistical weight matrix $\mathbf{U}$ (eq 6) would correspond to an 8×8 sparse matrix $\mathbf{U}_{8\times8}$, containing the transition probabilities of going from the triplet of bonds at the $(i-2)$th, $(i-1)$th, and ith positions along the chain in the isomeric rotational states X, Y, and Z to the next triplet of bonds at $(i-1)$th, ith, $(i+1)$th positions in the isomeric rotational states Y, Z, W. In our modeling only two possible isomeric rotational states are allowed for, i.e., X, Y, Z, $W = T^+$ or T^-. Then the 8×8 matrix can be written as eq A1.

The matrix $\mathbf{U}_{8\times8}$ can be reduced to a 3×3 matrix (eq 6), consistent with the fact that it is symmetric (i.e., elements $u_{ij} = u_{ji}$) and that triplets of bond states of kind $T^{\pm}T^{\mp}T^{\pm}$ or $T^{\mp}T^{\pm}T^{\mp}$ are forbidden.

The matrix of eq 6 may be obtained in a more straightforward way, associating to couples of consecu-

tive bonds symbol "l" if the two bonds are both T^+ or T^- (symbol "l" standing for "like) and symbol "u" if the two bonds have opposite sign (symbol "u" standing for "unlike"). As a consequence, of the four possible sequences "ll", "lu", "ul", and "uu", only the first three are possible. Then, the probability that a sequence of kind "ll" is followed by a sequence of kind "ll", "lu", or "ul" are 1, p, and 0, respectively, giving rise to the first row of eq 6; the probability that a sequence of kind "lu" is followed by a sequence of kind "ll", "lu", or "ul" is 0, 0, and 1, respectively, giving rise to the second row of eq 6; finally, the probability that a sequence of kind "ul" is followed by a sequence of kind "ll", "lu", or "ul" is 1, 0, and 0, respectively, giving rise to the third row of eq 6.

Acknowledgment. The Centro di Competenza "Nuove Tecnologie per le Attivita Produttive" Regione Campania P.O.R. 2000-2006 Misura 3.16 for financial support and the Centro Interdipartimentale di Metodologie Chimico Fisiche, University of Naples, are gratefully acknowledged.

References and Notes

(1) Sperati, C. A.; Starkweather, H. W., Jr. *Fortschr. Hochpolym. Forsch.* **1961**, *2*, 465.
(2) Pierce, R. H. H., Jr.; Clark, E. S.; Whitney, J. F.; Bryant, W. M. D. 130th Meeting of the American Chemical Society, Atlantic City, NJ, 1954; p 9.
(3) Bunn, C. W.; Howells, E. R. *Nature*, **1954**, *174,* 437.
(4) Clark, E. S.; Muus, L. T. *Z. Kristallogr*. **1962**, *117*, 119.
(5) Clark, E. S. *Bull. Am. Phys. Soc.* **1973**, *18*, 317.
(6) Clark, E. S. *Polymer* **1999**, *40*, 4659.
(7) Weeks, J. J.; Clark, E. S.; Eby, R. K. *Polymer* **1981**, *22*, 1480.
(8) Kilian, H. G. *Kolloid Z. Z. Polym.* **1962**, *185*, 13.
(9) Boerio, F. J.; Koenig, J. L. *J. Chem. Phys.* **1971**, *54*, 3667.
(10) Chantry, G. W.; Fleming, J. W.; Nicol, E. A.; Willis, H. A.; Cudby, M. E. A.; Boerio, F. J. *Polymer* **1974**, *15*, 69.
(11) Farmer, B. L.; Eby, R. K. *Polymer* **1985**, *26*, 1944.
(12) Yamamoto, T.; Hara, T. *Polymer* **1986**, *27*, 986.
(13) Corradini, P.; De Rosa, C.; Guerra, G.; Petraccone, V. *Macromolecules* **1987**, *20*, 3043.
(14) Corradini, P.; Guerra, G. *Macromolecules* **1977**, *10*, 1410.
(15) De Santis, P.; Giglio, E.; Liquori, A. M.; Ripamonti, A. *J. Polym. Sci. Part B* **1963**, *1*, 1383.
(16) Brown, R. G. *J. Chem. Phys.* **1964**, *40*, 2900.
(17) Clark, E. S. *J. Macromol. Sci. Phys.* **1967**, *1*, 795.
(18) Bates, T. W.; Stockmayer, W. H. *Macromolecules* **1968**, *1*, 12.
(19) Bates, T. W.; Stockmayer, W. H. *Macromolecules* **1968**, *1*, 17.
(20) D'Ilario, L.; Giglio, E. *Acta Crystallogr. Sci.* **1974**, *30*, 372.
(21) De Rosa, C.; Guerra, G.; Petraccone, V.; Centore, R.; Corradini, P. *Macromolecules* **1988**, *21*, 1174.
(22) Brown, R. G. *J. Chem Phys.* **1964**, *40*, 2900.
(23) Kimming, M.; Strobl, G.; Stün, B. *Macromolecules* **1994**, *27*, 2481.
(24) Matsushige, K.; Enoshita, R.; Ide, T.; Yamauch, N.; Take, S.; Takemura, T. *Jpn. J. Appl. Phys.* **1977**, *16*, 681.
(25) Yamamoto, T.; Hara, T. *Polymer* **1982**, *23*, 521.
(26) Frisch, M. J. et al. *Gaussian Development Version g03*; Gaussian Inc.: Pittsburgh, PA, 2003.
(27) Stewart, J. J. P. *J. Comput. Chem.* **1989**, *10*, 2, 209−220.
(28) Stewart, J. J. P. *J. Comput. Chem.* **1989**, *10*, 221.
(29) Cramer, C. J. *Essentials of Computational Chemistry;* John Wiley & Sons: New York, 2002.
(30) IUPAC Commission of Macromolecular Nomenclature. *Pure Appl. Chem.* **1981**, *53*, 733.
(31) Auriemma, F.; Petraccone, V.; Parravicini, L.; Corradini, P. *Macromolecules* **1997**, *30*, 7554.
(32) Tadokoro, H. *Structure of Cristalline Polymers;* John Wiley & Sons: New York, 1979.
(33) Allegra, G.; Bassi, I. *Gazz. Chim. Ital.* **1980**, *110*, 437. Allegra, G.; Bassi, I.; Meille, S. V. *Acta Crystallogr. A* **1978**, *34*, 653.
(34) Holt, D. B.; Farmer, B. L. *Polymer* **1999**, *40*, 4667−4672.
(35) Holt, D. B.; Farmer, B. L. *Polymer* **1999**, *40*, 4673−4681.
(36) Flory P. J. *Statistical Mechanics of Chain Molecules;* Interscience Publishers: New York, 1969.

MA0488257